Proceedings of the XXIII Conference on Applied Crystallography, Krynica Zdrój, Poland, September 20–24, 2015

Structure and Magnetic Properties of Amorphous $Fe_{82}Zr_7Nb_2Cu_1B_8$ and Crystalline $Fe_{82}Zr_6Y_1Nb_2Cu_1B_8$ Alloys

J. Gondro*, K. Błoch and M. Nabiałek

Częstochowa University of Technology, Institute of Physics, Faculty of Production Engineering and Materials Technology, al. Armii Krajowej 19, 42-200 Częstochowa, Poland

In order to obtain an alloy with a specific set of magnetic properties, the dominant influences of chemical component and thermal treatment selection need to be satisfied. In this paper, the results of investigations into the microstructure and magnetic properties of the following alloys are presented: amorphous $Fe_{82}Zr_7Nb_2Cu_1B_8$ and crystalline $Fe_{82}Zr_6Y_1Nb_2Cu_1B_8$. The structure and microstructure were examined using the Mössbauer spectroscopy and X-ray diffractometry. The $Fe_{82}Zr_7Nb_2Cu_1B_8$alloy was found to be fully amorphous in the as-quenched state and the transmission Mössbauer spectrum for this alloy is typical of that for weak ferromagnets, with an average hyperfine field of 9.86(2) T. The shape of this spectrum was found to have changed noticeably in the case of the $Fe_{82}Zr_6Y_1Nb_2Cu_1B_8$ alloy. This change was attributed to the presence of the crystalline phase bcc-Fe.

DOI: 10.12693/APhysPolA.130.909

PACS/topics: 75.47.Np, 75.50.Bb, 75.50.Kj, 75.90.+w

1. Introduction

The technique of ingot-rolling followed by heat treatment is one of the well-known methods for the preparation of conventional crystalline alloys [1–4]. For some time, there has been a dramatic increase in interest in electrotechnical materials with soft magnetic properties and amorphous or nanocrystalline structures. In order to prepare these materials, a suitable technique is used for rapid cooling of the material from the liquid phase. As a result of the rapid solidification of the melt, the following forms of material can be prepared: a tape having a thickness of several tens of μm, or rods, plates, tubes or other complicated shapes of materials having a thickness of several mm [5, 6].

When a large amount of energy (known as the activation energy of crystallization) is provided to an amorphous alloy, it tends to form seed crystals in the volume of the material, which leads later in their growth to the formation of crystallites of nanometric sizes [7–9].

Control of the heating process of amorphous alloys enables the production of an alloy with nanocrystalline structure [10–12]. Modern functional alloys, featuring amorphous and nanocrystalline structures, have a broad spectrum of applications [13]. In the case of soft ferromagnetic alloys with amorphous or nanocrystalline structures, very good magnetic characteristics are observed; this means that these alloys can be used in modern transformers, electric motors or microgenerators. In the amorphous alloys, it is possible to create a non-collinear magnetic structure together with fluctuations in the direction of easy magnetization, which is associated with the presence of various types of magnetic structures. Even in strong magnetic fields, such alloys do not reach ferromagnetic saturation. The presence of a complex magnetic structure within a single alloy can be observed in iron-based amorphous materials featuring the addition of zirconium [14, 15].

This paper presents microstructural and magnetic-ordering investigations for amorphous $Fe_{82}Zr_7Nb_2Cu_1B_8$ alloy; in addition, the effects are investigated of substituting 1 at.% weight of Zr for Y content in the composition of the alloy on the resulting microstructure and magnetic properties.

2. Experimental procedure

The samples used in this research were in the form of ribbons with a width of 3 mm and an approximate thickness of 20 μm. High-purity component chemicals were melted in an electric arc furnace, yielding ingots with the nominal compositions: $Fe_{82}Zr_7Nb_2Cu_1B_8$ and $Fe_{82}Zr_6Y_1Nb_2Cu_1B_8$. The desired amorphous ribbon samples were prepared by rapid cooling of the liquid metal on a single rotating copper cylinder (the melt-spinning process). An alloy sample containing yttrium was solidified on the cylinder at a rotational speed of 3800 rev./min and at a pressure of 0.03 MPa. The whole production process was undertaken under a protective atmosphere of argon. Microstructural and structural studies were performed on the samples in the post-solidification state, at room temperature. The microstructures of the produced materials were examined using a Mössbauer spectrometer and an X-ray diffractometer. A POLON Mössbauer spectrometer was used to observe the magnetic microstructure of the sample alloys; this spectrometer was equipped with a ^{57}Co (Rh) source, of 50 mCi activity. The transmission Mössbauer spectra were analysed using *NORMOS* software [16].

*corresponding author; e-mail: j.gondro@wp.pl

X-ray studies were carried out using a Brucker D8 Advance X-ray diffractometer. Experiments were undertaken within the 2θ-angle range from 30° to 130° with a measuring step-size of 0.02° and an exposure time of 7 s. Measurements were taken in the Bragg–Brentano geometry with a semiconductor counter and Cu K_α radiation.

Using the "Faraday balance", the magnetic properties of the materials were examined. Each investigated alloy sample was subjected to a magnetic field of 0.7 T, and then, using a TERMOS automated temperature controller, the sample was heated within the temperature range from 273 K to 850 K at a rate of 10 K/min. On the basis of the measurement points, the normalized thermomagnetic curves were determined, allowing the identification of the Curie temperature (T_C), according to the relationship

$$\left(\frac{M}{M_S}\right)^{1/\beta} = \left(\frac{M_0}{M_S}\right)^{1/\beta}\left(1-\frac{T}{T_C}\right), \qquad (1)$$

taking as β — critical exponent, equal to 0.36, for "Heisenberg" ferromagnetics [17, 18].

3. Results and discussion

The X-ray diffraction pattern for a sample of the alloy $Fe_{82}Zr_7Nb_2Cu_1B_8$ is shown in Fig. 1.

In this picture, pertaining to the sample in the post-solidification state, no narrow peaks (which would correspond to a crystalline phase) can be seen. The resulting diffraction pattern shows a broad halo at a 2Θ-angle of approximately 50°, which is typical for amorphous alloys featuring an iron matrix.

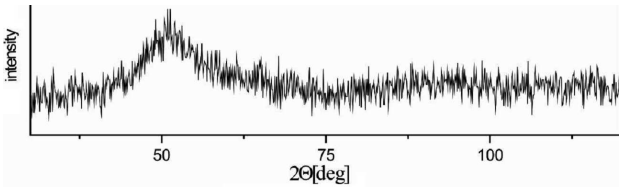

Fig. 1. X-ray diffraction pattern for the sample of $Fe_{82}Zr_7Nb_2Cu_1B_8$ alloy in the as-quenched state.

The amorphousness of the investigated alloy was further confirmed by the Mössbauer studies (Fig. 2).

The Mössbauer transmission spectra and hyperfine field distribution, obtained for the alloy $Fe_{82}Zr_7Nb_2Cu_1B_8$ in the post-solidification state, are shown in Fig. 2. The shape of the spectrum is characteristic of that expected for a ferromagnetic amorphous alloy of high iron content [19].

The spectrum consists of broad overlapping lines indicating a disordered alloy structure. In the hyperfine field induction distribution it is possible to distinguish a low-field component responsible for the presence of a high concentration of iron atoms with small distances between them. A high-field component, which can be observed at higher fields of the hyperfine field distribution on the iron nuclei, gives an indication of the presence

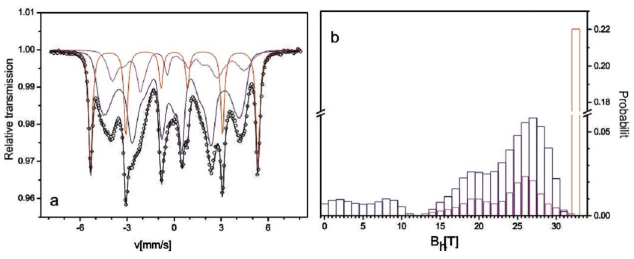

Fig. 2. Transmission Mössbauer spectra (a) and derived hyperfine field distribution (b) for the $Fe_{82}Zr_7Nb_2Cu_1B_8$ amorphous alloy in the as-quenched state.

of other elements such as Zr or B near the iron atoms. From analysis of the Mössbauer spectra (Table I) it can be concluded that the intensity of the second line in the Zeeman sextet is 2.7, which means that the magnetization vector of the ribbon is positioned perpendicular to the surface.

TABLE I

The average hyperfine field at ^{57}Fe nuclei $(B_{hf})_{ef}$ and the intensity of the second line in the Zeeman sextets ($A_{2,5}$) for the investigated samples in the as-quenched state.

Sample (asq)	$B_{hf_{ef}}$ [T]	ΔD_S [T]	$A_{2.5}$
$Fe_{82}Zr_7Nb_2Cu_1B_8$	9.86(2)	4.17(2)	2.7(1)
$Fe_{82}Zr_6Y_1Nb_2Cu_1B_8$	14.82(2)	4,71(2)	4.0 (1)

In the case of an alloy containing yttrium (Fig. 3) the intensity of the $A_{2.5}$ line is 4, which indicates that the vector of magnetization is set parallel to the ribbon surface.

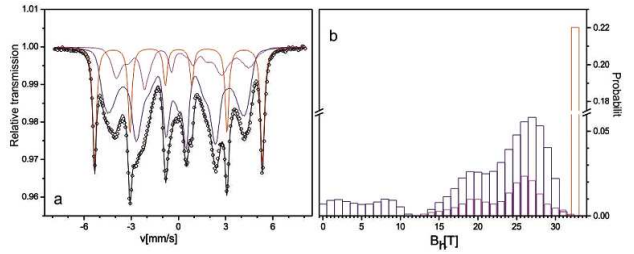

Fig. 3. Transmission Mössbauer spectra (a) and derived hyperfine field distributions (b) for the $Fe_{82}Zr_6Y_1Nb_2Cu_1B_8$ amorphous alloy in the as-quenched state.

The X-ray diffraction pattern, measured for a sample of the $Fe_{82}Zr_6Y_1Nb_2Cu_1B_8$ alloy in the post-solidification state, is shown in Fig. 4.

Within the resulting pattern, distinct peaks are visible, which testify to the presence of a crystalline phase. The sharp peaks that are visible in the X-ray diffraction pattern were identified through the use of a specialized PDF database. This allowed specific phases to be assigned to the crystalline peaks (Fig. 4).

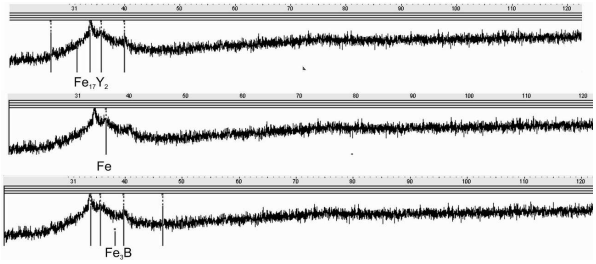

Fig. 4. X-ray diffraction pattern with marked phases for the sample of $Fe_{82}Zr_6Y_1Nb_2Cu_1B_8$ alloy in the as-quenched state.

Figure 3a shows the Mössbauer spectrum together with the hyperfine field distribution (Fig. 3b) measured at room temperature for the $Fe_{82}Zr_6Y_1Nb_2Cu_1B_8$ alloy in the post-solidification state. The shape of this spectrum has clearly changed: narrow lines are visible, corresponding to the crystalline phase bcc-Fe. For the sample of alloy containing yttrium in its composition, an increase in the average hyperfine field induction was observed; this is associated with the distance between the iron atoms and their presence within the near neighbourhood of atoms of other elements — in this case, yttrium atoms. The increase of the $(B_{hf})_{ef}$ parameter for the $Fe_{82}Zr_6Y_1Nb_2Cu_1B_8$ sample reveals an increased density of atoms, compared with the alloy that did not contain 1 at.% of Y.

Measurements of magnetization as a function of temperature allowed the Curie temperatures of the investigated alloys to be determined. Figure 5 shows specific magnetization curves (σ) as a function of temperature under constant magnetizing field (0.75 T) for the examined alloys.

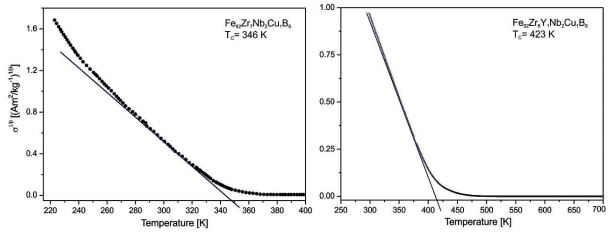

Fig. 5. Dependence of the specific magnetization on temperature for the investigated samples in the as-quenched state.

Magnetization for both of the investigated alloys gradually decreases with temperature, but does not reach zero. The Curie temperature for the alloy containing yttrium is much higher (T_C = 423 K). This fact is related to the presence in the alloy of the crystalline phase and the replacement of zirconium atoms by yttrium atoms. Yttrium has a larger atomic radius (r_Y = 0.180 nm) compared with the atomic radius of zirconium (r_{Zr} = 0.155 nm). This difference in radius affects the arrangement of atoms within the volume of the alloy and, in turn, affects the resulting magnetic properties — which may be manifested as the higher Curie temperature of the $Fe_{82}Zr_6Y_1Nb_2Cu_1B_8$ alloy. The addition of yttrium restricts the free movement of atoms due to the size mismatch between Zr and Y [20]. On the other hand, the increased Curie temperature (T_C = 423 K) of the alloy containing Y (relative to the composition $Fe_{82}Zr_7Nb_2Cu_1B_8$, for which T_C = 346 K) should be associated with an increase in the exchange integral J_r.

4. Conclusions

In conclusion, it may be stated that the multicomponent $Fe_{82}Zr_7Nb_2Cu_1B_8$ alloy in the as-quenched state was fully amorphous. The X-ray diffraction pattern, presented for the $Fe_{82}Zr_6Y_1Nb_2Cu_1B_8$ alloy sample, shows clear peaks indicating the presence of a crystalline phase. The increase in the average magnetic hyperfine induction field for the $Fe_{82}Zr_6Y_1Nb_2Cu_1B_8$ alloy sample is associated with the larger distance between the iron atoms therein and the presence in their near neighbourhood of other chemical elements — in this case, yttrium atoms. The Curie temperature of the sample with added yttrium is much higher (T_c = 423 K) than that for the $Fe_{82}Zr_6Y_1Nb_2Cu_1B_8$ alloy (T_C =346 K). The addition of yttrium restricts the free movement of atoms due to the size mismatch between Zr and Y.

The ribbon samples investigated during this work were prepared using the same method and under the same conditions. This fact confirms the theory that even minor changes in the chemical composition of an alloy can significantly change the resulting magnetic properties.

References

[1] A.P. Thomas, M.R.J. Gibbs, *J. Magn. Magn. Mater.* **103**, 97 (1992).

[2] M. Hasiak, K. Sobczyk, J. Zbroszczyk, W. Ciurzyńska, J. Olszewski, M. Nabiałek, J. Kaleta, J. Świerczek, A. Łukiewska, *IEEE Trans. Magn.* **11**, 3879 (2008).

[3] K. Sobczyk, J. Świerczek, J. Gondro, J. Zbroszczyk, W. Ciurzyńska, J. Olszewski, P. Brągiel, A. Łukiewska, J. Rzącki, M. Nabiałek, *J. Magn. Magn. Mater.* **324**, 540 (2012).

[4] P. Pawlik, M. Nabiałek, E. Żak, J. Zbroszczyk, J.J. Wysłocki, J. Olszewski, K. Pawlik, *Archiv. Mater. Sci.* **25**, 177 (2004).

[5] M. Nabiałek, *J. Alloys Comp.* **642**, 98 (2015).

[6] K. Błoch, *J. Magn. Magn. Mater.* **390**, 118 (2015).

[7] S.N. Kane, S. Sarabhai, A. Gupta, L.K. Varga, T. Kulik, *J. Magn. Magn. Mater.* **215-216**, 372 (2000).

[8] M. Al-Haj, J. Barry, *J. Mater. Sci. Lett.* **17**, 1125 (1998).

[9] K. Błoch, M. Nabiałek, M. Dośpiał, S. Garus, *Archiv. Metall. Mater.* **60**, 7 (2015).

[10] T. Egami, *J. Magn. Magn. Mater.* **31-34**, 1571 (1983).

[11] D. Szewieczek, S. Lesz, *J. Mater. Process. Technol.* **162-163**, 254 (2005).

[12] T. Kozieł, A. Zielińska-Lipiec, Z. Kędzierski, T. Czeppe, *J. Microsc.* **224**, 27 (2006).

[13] Y. Takahara, *Mater. Sci. Eng. A* **231**, 128 (1997).

[14] J. Gondro, J. Świerczek, J. Rzącki, W. Ciurzyńska, J. Olszewski, J. Zbroszczyk, K. Błoch, M. Osyra, A. Łukiewska, *J. Magn. Magn. Mater.* **341**, 100 (2013).

[15] H. Kronmüller, *Philos. Mag.* **48**, 127 (1983).

[16] A. Brand, *Nucl. Instrum. Methods Phys. Res. B* **28**, 398 (1987).

[17] D.H. Ryan, J.M.D. Coey, E. Batalla, Z. Altouniam, J.O. Ström-Olsen, *Phys. Rev. B* **35**, 8630 (1987).

[18] S.N. Kaul, V. Siruguri, G. Chandra, *Phys. Rev. B* **45**, 12343 (1992).

[19] R. Meyer, H. Kronmüller, *Phys. Status Solidi B* **109**, 693 (1982).

[20] I. Betancourt, S. Baez, *J. Non-Cryst. Solids* **355**, 1202 (2009).